Published online August 3, 2006

Including Topography and Vegetation Attributes for Developing Pedotransfer Functions

Sanjay K. Sharma, Binayak P. Mohanty,* and Jianting Zhu

ABSTRACT

With the advent of advanced geographical informational systems (GIS) and remote sensing technologies in recent years, topographic (elevation, slope, aspect, and flow accumulation) and vegetation attributes are routinely available from digital elevation models (DEMs) and normalized difference vegetation index (NDVI) at different spatial (remote sensor footprint, watershed, regional) scales. Based on the correlation of soil distribution and vegetation growth patterns across a topographically heterogeneous landscape, this study explores the use of topographic and vegetation attributes in addition to pedologic attributes to develop pedotransfer functions (PTFs) for estimating soil hydraulic properties in the Southern Great Plains of the USA. The extensive Southern Great Plains 1997 (SGP97) hydrology experiment database was used to derive these functions by using artificial neural networks. Eighteen models combining bootstrapping technique with artificial neural networks were developed in a hierarchical manner to predict the soil water contents at eight different soil water potentials (θ at 5, 10, 333, 500, 1000, 3000, 8000, and 15000 cm) and the van Genuchten hydraulic parameters (θ_r, θ_s, α, n). The performance of the neural network models was evaluated using the Spearman correlation coefficient between the observed and the predicted values and root mean square error (RMSE). Although variability exists within bootstrapped replications, improvements (of different levels of statistical significance) were achieved with certain input combinations of basic soil properties, topography and vegetation information compared with using only the basic soil properties as inputs. Topography (DEM) and vegetation (NDVI) attributes at finer scales were useful to capture the variations within the soil mapping units for the SGP97 region dominated by perennial grass cover.

Global- and regional-scale circulation models including soil vegetation atmosphere transfer (SVAT) schemes are routinely used by many for hydrologic and climate forecasting. Besides, numerical models are used at the catchment–watershed scales for simulating water and chemical transport in surface, vadose zone, and ground water systems. The accuracy of the input parameters used in these models such as soil hydraulic properties has a significant effect on model results. Lack of detailed input data sets for these models is a major limitation for simulation of hydrologic processes at the regional scales. Direct measurements of soil hydraulic properties are time-consuming and costly to characterize large regions. They also require collecting large number of undisturbed soil samples or in situ measurements to account for the inherent spatial variability of soil properties. Indirect estimation techniques using PTFs provide an effective alternative to the direct measurements. A number of studies have been performed in the past decades in developing such functions and testing them against available soil properties databases (e.g., Rawls et al., 1991; van Genuchten and Leij, 1992; Pachepsky et al., 1999; Wösten et al., 2001). Based on the model and the predicted outputs, the PTFs can be classified into "point regression method" that predict the soil water content at fixed soil water potentials in the water retention curve based on empirically derived regression equations (e.g., Rawls et al., 1982; Ahuja et al., 1985; Tomasella et al., 2000) and "function parameter method" that predict the parameters of the hydraulic property functions (e.g., Vereecken et al., 1989; Schaap et al., 1998; Wösten et al., 2001) such as those given by Brooks and Corey (1964), Campbell (1974), and van Genuchten (1980). Both approaches have been widely employed for various soil databases. Parametric approach was found to be usually preferable than predicting water retention at specific potentials, as it generates a continuous function of the $\theta(h)$ relationship. Water retention at any potential can be estimated with these functions. In a recent study, both the point-based and parameter-based methods were used simultaneously for colocated information on soil basic properties and water retention data for Brazilian soils encompassing diverse textural classes (Tomasella et al., 2003). Comparison of results between the two methods indicated better performance for point-based approach over parameter-based approach suggesting water content in Brazilian soils was controlled by different independent variables at different water potentials including soil structure, texture, and organic matter. In other words, some basic soil properties are more important in the wet range of water retention curve, while other properties control the water retention variability in the dry range. Contrarily, shape parameters of the analytical water retention curve describe its behavior both in wet and dry range resulting in poor performance of parameter-based approach because of its inaccuracy to capture the complexity of the soil system.

Soil texture has been widely used to predict the soil hydraulic properties. Using detailed particle-size distributions (PSD) has been shown to increase the accuracy of soil hydraulic parameters predictions (Schaap et al., 1998) compared with predictions from textural class alone (Clapp and Hornberger, 1978). Most commonly used soil physical properties for prediction of the soil hydraulic properties are soil texture, organic carbon (OC), and bulk

S.K. Sharma, currently at Dep. of Agricultural and Food Engineering. IIT Kharagpur, West Bengal, India 721302; B.P. Mohanty, Biological and Agric. Engineering, 2117 TAMU, 301C Scoates Hall, Texas A&M Univ., College Station, TX 77843-2117; J. Zhu, currently at Desert Research Institute, 755 E. Flamingo Rd., Las Vegas, NV 89119. Received 22 Mar. 2005. *Corresponding author (bmohanty@tamu.edu).

Published in Soil Sci. Soc. Am. J. 70:1430–1440 (2006).
Soil Physics
doi:10.2136/sssaj2005.0087

677 S. Segoe Rd., Madison, WI 53711 USA

Abbreviations: CF, Central Facility; DEMs, digital elevation models; ER, El Reno; GIS, geographical information system; LW, Little Washita; OC, organic carbon; PSD, particle size distribution; PTF, pedotransfer function; PTVTF, pedo-topo-vegetation transfer function; NDVI, normalized difference vegetation index; SGP97, Southern Great Plains 1997 hydrology experiment; SVAT, soil vegetation atmosphere transfer.

density (ρ_b). Additional parameters were rarely used in developing PTFs (Wösten et al., 2001). Recently, Pachepsky et al. (2001) and Leij et al. (2004) included more-readily available topographical attributes in addition to soil physical parameters to develop PTFs for hill-slopes in Maryland, USA, and Basilicata, Italy, respectively. The results of their studies indicated improvement in the performance of PTFs in predicting soil hydraulic properties by the inclusion of topographical attributes such as slope, elevation, curvature, aspect, and potential solar radiation. Pachepsky et al. (2001) developed regression equations relating topographical variables calculated from DEM across a 3.7-ha gently sloping land to soil water retention at 10, 33, and 100 KPa, the results of which showed the potential of using topographical attributes as input parameters in these functions. Leij et al. (2004) developed relationships for van Genuchten fitting parameters (α, n, θ_s, θ_r, K_s) and water retention at 5 and 1200 KPa using both basic soil properties and topographical attributes on a 5 km-long hill-slope transect. While the results from both studies are promising, the main limitations are that a soil sample were taken along one or more transects and thus were limited to a specific hillslope or catchment scale.

With the increasing availability of remote sensing products from air- and space-borne sensors at different spatial resolutions, additional land surface parameters can be explored for their utility in developing/improving catchment- or regional-scale PTFs. Based on relationships of soil OC with land use and vegetation cover, we explored the usefulness of remotely sensed NDVI in addition to soil physical and topographical attributes for the estimation of soil hydraulic properties across the southern Great Plains region of the USA, dominated by perennial grass cover. The influence of vegetation attributes such as vegetation type, density, and uniformity on soil (moisture retention) properties have been observed and recognized in the past (Reynolds, 1970; Hawley et al., 1983). More recently, Mohanty et al. (2000) showed the influence of vegetation dynamics controlling the intraseasonal soil moisture spatial structure. Mohanty and Skaggs (2001) also showed that the combination of soil properties, topographic features, and vegetation attributes jointly govern the temporal structures (including central tendency and distribution) of soil moisture during the SGP97 remote sensing hydrology experiment. In this study, we hypothesize that vegetation has indirect effect on soil hydraulic properties and soil pore development and thus has the potential of being used as a possible input for PTFs along with soil and topographical attributes. A novel feature of this study is to extend PTFs to PTVTFs by addition of information on topography using DEM and vegetation information from NDVI. The primary objective of the study is to develop and examine the performance of hierarchical PTVTFs for the Southern Great Plains region of USA using ground-based (soil), DEM-based (topography), and remotely sensed (vegetation) databases collected during the SGP97 hydrology experiment. This study also demonstrates the differences in the mapping of hydraulic parameters for LW watershed based on the type of inputs used for transfer functions. Note that disparity in measurement/support scales between soil hydraulic properties (<10 cm) and county soil survey (30 m), DEM (30 m), or NDVI (30 m) databases is not the main focus of this paper and is thus ignored.

MATERIALS AND METHODS

General Site Description

Soil property data from SGP97 remote sensing hydrology experiment was used in the study. The data are the result of an extensive soil property campaign performed concurrently with large scale multi platform remote sensing measurements that make it possible to develop PTVTFs for the region. The SGP97 remote sensing hydrology experiment was sponsored by the National Aeronautic and Space Administration (NASA) and cosponsored by United States Department of Agriculture–Agricultural Research Service (USDA-ARS), National Oceanic and Atmospheric Administration (NOAA), Department of Energy (DOE), National Science Foundation (NSF), and other federal and state agencies. The experiment covered a region of approximately 40 km by 250 km (10000 km^2) within the central part of the U. S. Great Plains in the subhumid environment of Oklahoma with a north-south precipitation gradient (Famiglietti et al., 1999). Soils include a wide range of textures with large areas of both coarse and fine textures (STATSGO database, National Resources Conservation Service [NRCS]; county soil survey). The topography of the region is moderately rolling. Rangeland and pasture with significant areas of winter wheat and other crops dominate land use. Additional background information on the Little Washita (LW) watershed in the southern part of the SGP97 region can be found in Allen and Naney (1991) and Jackson and Schiebe (1993). Other relevant surface hydrometeorological, vegetation, soil, and topographic information for the SGP97 region can be accessed at http://daac.gsfc.nasa.gov/fieldexp/SGP97 (verified 3 May 2006).

Soil Attributes

We collected soil cores from different depths at representative (soil, topography, and vegetation) sites based on a priori information (gleaned from digital maps and overlays, http://www.cei.psu.edu/nasa_lsh/) and concurrent site inspection. Although in the database (Mohanty et al., 2002) we provided more detailed and unbounded site classifications for future studies reference, various combinations among soil texture (12 USDA classes, Fig. 15–03, Gee and Bauder, 1986), relative position (valley, hill-slope, hill-top), and vegetation type (grass, shrub, crop) were used as the primary groups for our site selection protocol. A total of 157 soil cores (in brass cylinders, 5.3 cm diameter and 5.9 cm height) were collected from 46 quarter sections (800 m $\times$ 800 m) matching the air-borne electronically scanned thinned array radiometer (ESTAR) footprints within the Little Washita (LW), El Reno (ER), and Central Facility (CF) intensive study areas (Fig. 1). While most soil cores were collected near the soil surface (3- to 9-cm depth), a few cores were collected at deeper depths (within top 1 m) to encompass the entire root zone important for available water for the plant growth. Soil cores were analyzed in the laboratory for PSD, bulk density, OC, soil water retention, dynamic outflow, and saturated and unsaturated hydraulic conductivities. Details of the sampling plan, field procedures, and laboratory measurement methods are given in Mohanty et al. (2002) and available online at http://daac.gsfc.nasa.gov/fieldexp/SGP97. Soil texture distribution across LW, ER and CF intensive study areas based on the particle size distribution measurements of soil samples are shown in Fig. 2.

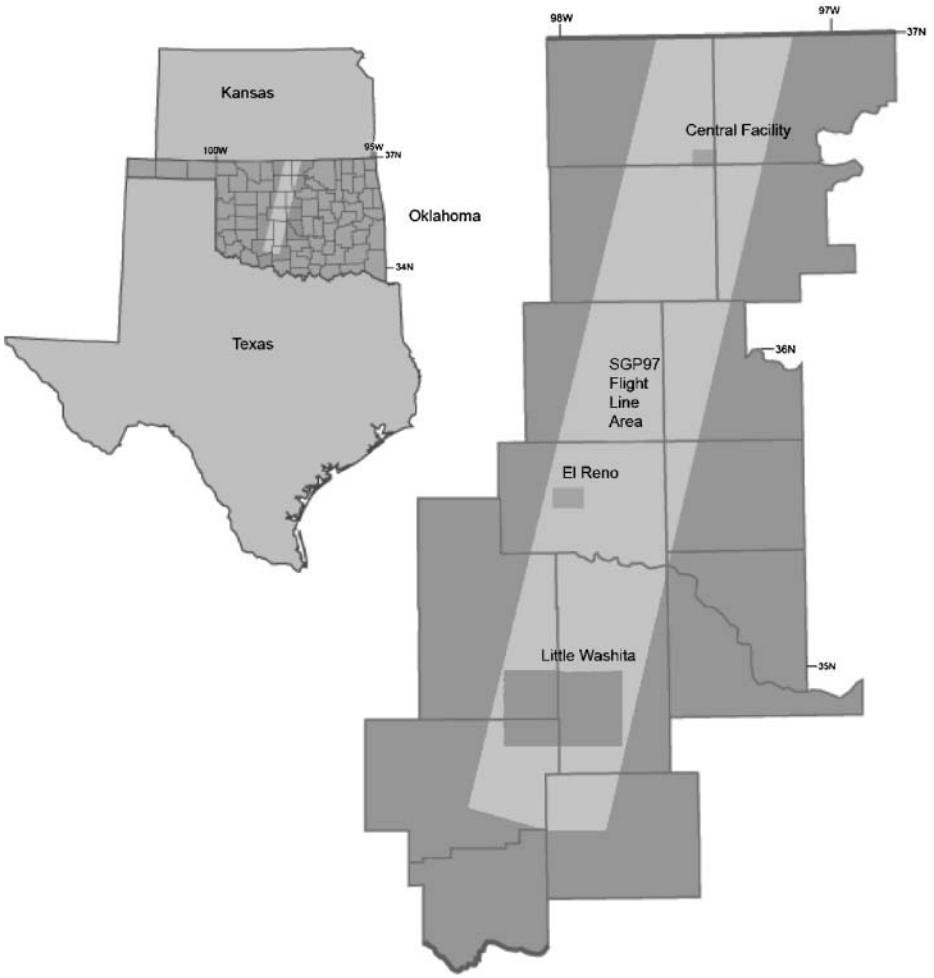

Fig. 1. Geographical location of Southern Great Plains 1997 (SGP97) Hydrology Experiment in Oklahoma.

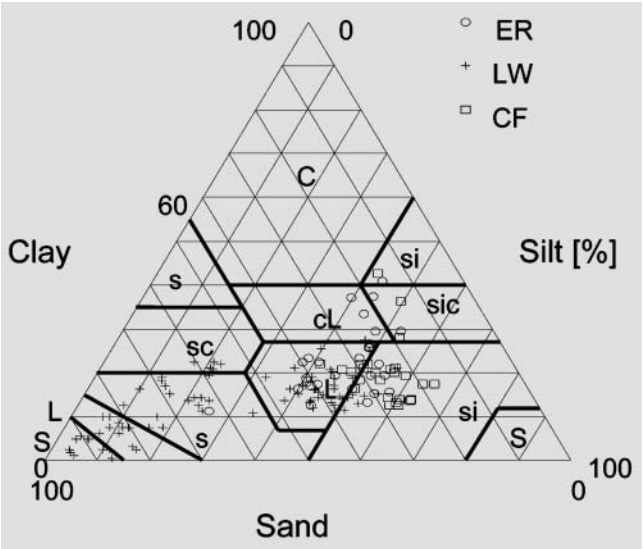

Fig. 2. Soil texture distribution across the Little Washita (LW), El Reno (ER), and Central Facility (CF) focus regions based on particle size distribution (PSD) measurements of 157 samples.

Topographic Attributes

The topography of the study site was characterized with DEMs of 30 m by 30 m resolution for LW, ER and CF areas (http://www.cei.psu.edu/nasa_lsh/). The topographic attributes including elevation, slope, aspect, and flow accumulation were calculated using Arc View software (ver 3.2). Other secondary attributes like profile/plan curvature were omitted due to their low order of magnitudes (10^{-3}). The slope (in degree) represents the maximum rate of change of elevation between each cell and its neighbors. Aspect represents the direction of slope. It identifies the maximum rate of change in down-slope direction. The flow accumulation represents the volume of water that is collected in the study cell/grid. Areas with stream channels have maximum flow accumulation while the ridges reflect zero flow accumulation. Using raster GIS, flow accumulation for each cell/grid is simply determined by the number of adjacent cells/grids flowing into it.

Vegetation Attribute

The NDVI was used to quantify the vegetation in each remote sensing footprint/pixel. The NDVI is a greenness index that is related to the proportion of photosynthetically absorbed radiation and reflects the chlorophyll activity in plant. Within a remote sensing footprint/pixel, an increase in NDVI value signifies an increase of green vegetation. During the SGP97 remote sensing hydrology experiment, NDVI for the

study region was derived using Landsat-7 Thematic Mapper (TM) on 25 July 1997 at a spatial resolution of 30 m by 30 m. The SGP97 remote sensing/ground vegetation datasets can be located at http://daac.gsfc.nasa.gov/data/sgp97/vegetation/ndvi/. In this study area, dominated by perennial grass cover, we assumed that the vegetation distribution across the SGP region remained constant across time based on the 25 July 1997 TM snap shot. The value of NDVI ranges from −1 to +1 with vegetated areas typically having values greater than zero. The NDVI estimates can be considered as an indirect indicator of amount of biomass added to the soil surface which may be related to the OC content of the soil. Changes in NDVI also correspond to the changes in the vegetation health thus hinting at the plant available water, and in turn the bulk density, pore size/structure evolution, and the hydraulic properties (soil water retention and hydraulic conductivity) of soil.

Neural Network Analysis

Information from the elevation, slope, aspect, flow accumulation, and NDVI grids was interpolated and combined with soil information collected from the soil cores by utilizing the Grid Utility functions in ArcView. Different models using different combination of soil-topography-vegetation attributes as input were developed to predict soil hydraulic parameters for the widely used van Genuchten (1980) functional relationship and water content at eight different soil water matric potentials (i.e., 5, 10, 333, 500, 1000, 3000, 8000, 15000 cm). The van Genuchten soil hydraulic function (van Genuchten, 1980) is defined as:

$$\theta(h) = \theta_r + \frac{\theta_s - \theta_r}{[1 + (\alpha h)^n]^m} \quad [1]$$

where h is the soil water matric potential [L], θ is the soil water content [L^3L^{-3}], θ_r is the residual water content of the soil [L^3L^{-3}], θ_s is the saturated water content of the soil [L^3L^{-3}], α is a shape factor, approximately equal to the inverse to the air entry value [L^{-1}], n is a pore-size distribution index [-], and m is an empirical constant that can be related to n (e.g., $m = 1 - 1/n$). Table 1 shows the basic statistics of the input and output variables including van Genuchten parameters (α, n, θ_s and θ_r) and water content at different matric potentials (θ at 5, 10, 333, 500, 1000, 3000, 8000, and 15000 cm) predicted by the PTVTFs.

Feedforward and backpropagation type of neural networks are generally used to develop PTFs (Pachepsky et al., 1996; Schaap et al., 1998; Koekkoek and Booltink, 1999). Pedotransfer functions for different hierarchical levels of input parameters were also developed using neural networks (Schaap et al., 1998). In this study, neural network analysis was performed using the *Neuropath* Software (Minasny and McBratney, 2002). A neural network comprises of a set of simple computing elements (neurons), which are organized as layers and are linked together by weights. A neural network typically consists of an input layer, an output layer and one or more hidden layers linking the two layers. The hidden layer extracts useful information from inputs and uses them to predict the outputs. Following Schaap et al. (1998), the number of neurons in the hidden layer was set to six. The mathematical representation of a neural network model consists of a set of simple functions linked together by weights. A network with an input vector of elements x_l ($l = 1, \ldots, Ni$) is transmitted through a connection that is multiplied by weight W_{jl} to give the hidden unit z_j ($j = 1, \ldots, Nh$):

$$z_j = \sum_{l=1}^{Ni} w_{jl} + w_0 \quad [2]$$

where Nh is the number of hidden units and Ni is the number of input units. The hidden units consist of the weighted input (w_{jl}) and a bias (w_o). A bias of input equal to 1 that serves as a constant added to the weight. These inputs are passed through a layer of activation function f, which are designed to accommodate the nonlinearity in the input-output relationships. The function used in *Neuropath* is the sigmoid or hyperbolic tangent:

$$f(z) = \tanh(z) = 1 - \frac{2}{1 + \exp(2z)} \quad [3]$$

The outputs from hidden units pass another layer of filters with weights (u_{kj}) and bias ($u0$) and are fed into another activation function F to produce output y ($k = 1, \ldots, N_o$):

$$y_k = F\left[\sum_{j=1}^{N_h} u_{kjf}\left(\sum_{l=1}^{N_l} w_{jl} + w_o\right) + u_o\right] \quad [4]$$

The weights are adjustable parameters of the network and are determined from a set of data through the process of training. The NL2SOL adaptive nonlinear least squares algorithm (Dennis et al., 1981) implemented in the *Neuropath* software was used for training of networks by minimizing the sum of squares of the residuals between the measured and predicted outputs.

$$\mathbf{O}(W,U) = \sum_{i=1}^{Ns}\sum_{k=1}^{No}(\widehat{P}_{ik}(X_i) - P_{ik})^2 \quad [5]$$

where N_s is the number of samples, N_o is the number of outputs, W and U are weights of the hidden and the output layer, respectively, P_{ik} is the measured output and $\widehat{P}$ (X) is the predicted output [i.e., θ_r, θ_s, α, n, or $\theta(h)$] from the inputs X.

Neural networks have been combined with the bootstrap method in the software. The bootstrap method (Efron and Tibshirani, 1993) helps to obtain an estimate of the uncertainty in the predictions of neural networks by resampling the training and validation data. Bootstrap assumes that the training data set is a representation of the population, and multiple realizations of the population can be simulated from a single dataset. This is done by repeated 'sampling with replacement' of the original dataset of size N to obtain B bootstrap data sets, each with the size N. Further details of the combined neural network-bootstrapping approach adopted here can be found in Schaap et al. (1998).

A total of 140 (out of 157) soil samples containing all the input information of soil, topography and vegetation attributes

Table 1. Basic statistics of the inputs and outputs parameters.

	Mean	Standard deviation	Minimum	Median	Maximum
SAND %	45.193	24.115	1.480	37.858	94.043
SILT %	37.228	17.800	3.457	43.699	65.179
CLAY %	17.579	9.275	0.636	16.687	43.750
BD g cm^{-3}	1.408	0.104	1.074	1.411	1.711
NDVI ratio	0.271	0.248	−0.380	0.350	0.630
DEM m	378.319	43.891	302.000	392.965	444.000
OC %	0.782	0.488	0.130	0.665	2.140
SLOPE, degree	0.035	0.029	0.000	0.036	0.111
ASPECT, degree	165.878	87.859	0.000	167.0	347.0
FLOWACC	29.631	195.624	0.00	2.0	2128.0
θ_r	0.088	0.049	0.000	0.084	0.211
θ_s	0.372	0.051	0.251	0.367	0.703
A	0.016	0.010	0.002	0.014	0.077
N	1.721	0.909	1.102	1.507	7.513
θ_5	0.358	0.039	0.249	0.355	0.473
θ_{10}	0.356	0.039	0.249	0.353	0.469
θ_{333}	0.228	0.066	0.049	0.243	0.382
θ_{500}	0.208	0.067	0.044	0.219	0.368
θ_{1000}	0.180	0.065	0.036	0.185	0.357
θ_{3000}	0.146	0.060	0.026	0.143	0.318
θ_{8000}	0.128	0.053	0.021	0.127	0.311
θ_{15000}	0.126	0.056	0.021	0.121	0.309

Table 2. Correlation coefficients (*r*) between the input and output hydraulic parameters.†

	SAND	SILT	CLAY	OC	BD	NDVI	DEM	SLOPE	ASPECT	FLCC	θ_r	θ_s	α	n
SAND	1.000	−0.866	−0.790	−0.375	0.311	−0.163	0.252	0.572	0.067	−0.336	−0.142	−0.371	0.059	0.575
SILT		1.000	0.484	0.476	−0.470	0.096	−0.377	−0.486	−0.038	0.334	0.129	0.340	−0.164	−0.479
CLAY			1.000	0.239	−0.089	0.151	−0.052	−0.392	−0.117	0.124	0.247	0.361	0.090	−0.581
OC				1.000	−0.442	−0.118	−0.145	−0.133	−0.085	0.110	0.161	0.339	−0.062	−0.375
BD					1.000	−0.079	0.181	0.177	0.077	−0.182	−0.102	−0.593	−0.162	0.114
NDVI						1.000	0.096	−0.253	0.102	0.173	0.213	0.125	0.091	−0.077
DEM							1.000	−0.111	0.339	−0.206	0.129	−0.051	0.215	0.040
SLOPE								1.000	−0.288	−0.103	0.042	−0.271	−0.096	0.299
ASPECT									1.000	−0.079	−0.027	−0.110	0.082	0.007
FLOWACC										1.000	0.067	0.219	−0.051	−0.164
θ_r											1.000	0.068	−0.068	0.083
θ_s												1.000	0.337	−0.320
α													1.000	−0.222
n														1.000

† Significant correlations are underlined.

were chosen for this study. The data was split into two sets (i.e., training and validation). Each training set of 100 soil samples was obtained from a total of 140 by random resampling and the other 40 soil samples were used as the validation set. Thirty random replications of training and validation sets were used for bootstrapping. The final output was generated by bootstrap aggregation in *Neuropath*, which averages each bootstrap estimates from all the iterations. The number of iterations for each prediction was set to 100. The 5 and 95 percentiles of the estimates calculated by *Neuropath* was used to determine the uncertainty of the predictions.

Separate sets of neural network models were used to predict the van Genuchten hydraulic parameters (θ_r, θ_s, α, *n*) and the water contents at different matric potentials θ(*h*). This is because PTFs that showed improved predictions for one of the van Genuchten parameters does not necessarily perform better in predicting the water contents at different matric potentials (Schaap et al., 1998). This was attributed to the nonlinear nature of the hydraulic functions.

Based on the preliminary analysis of correlation coefficients (Tables 2 and 3), 18 different neural network models following a hierarchical approach of inputs were developed for the van Genuchten hydraulic parameters and soil water contents at different matric potentials. The model inputs were arranged in hierarchy as shown in Table 4. The inputs for Model 1 to 3 were based solely on basic soil properties (i.e., %sand, %silt, %clay, OC, and bulk density). Model 4 to 13 used an additional single topographic or vegetation attribute along with basic soil properties. Model 14 to 17 were built by combining one topographic feature with vegetation and soil properties. Finally, Model 18 was formed by including all the soil, vegetation and topographic attributes for prediction of hydraulic parameters and water content at different matric potentials. Performance of the neural network models was evaluated by spearman's correlation coefficient (*r*) and root mean square error (RMSE) between the measured and the estimated values.

$$\mathrm{RMSE} = \sqrt{\frac{\sum_{i=1}^{N}(y_i - y_i')^2}{N}} \qquad [6]$$

where *N* is the number of samples, y_i and y_i' are the optimized/measured (based on lab measurements of field samples) and predicted (by neural networks) output variables, respectively.

RESULTS AND DISCUSSION

Table 2 shows the correlation coefficients between the different predictors and the van Genuchten hydraulic parameters (θ_r, θ_s, α, *n*). Residual water content, θ_r, showed significant correlation only with %clay and NDVI. Physically, this may illustrate the inherent relationship between the fine particles, small pore sizes, adsorbed water, and available water (between field capacity and permanent wilting point/residual water content) to the plants as reflected in their greenness. On the contrary, saturated water content, θ_s, showed significant correlation with all the basic soil properties (i.e., %sand, %silt, %clay, OC, and bulk density) and with slope and flow accumulation among the topographic attributes. This finding suggests a relationship of θ_s as a function of soil PSD and depositional pattern across the landscape as a result of soil genesis and/or anthropogenic changes. The fitting parameter, α, did not show any significant correlation with any of the input parameters except elevation. On the other hand, fitting parameter *n* followed the same trend as θ_s and

Table 3. Correlation coefficients (*r*) between the inputs and output water contents at matric potentials.†

	θ_5	θ_{10}	θ_{333}	θ_{500}	θ_{1000}	θ_{3000}	θ_{8000}	θ_{15000}
SAND	−0.439	−0.445	−0.444	−0.449	−0.402	−0.378	−0.360	−0.282
SILT	0.401	0.406	0.445	0.444	0.391	0.354	0.317	0.262
CLAY	0.354	0.354	0.330	0.345	0.313	0.31	0.310	0.208
OC	0.308	0.312	0.293	0.278	0.220	0.163	0.139	0.218
BD	−0.145	−0.144	−0.330	−0.348	−0.324	−0.276	−0.245	−0.221
NDVI	0.017	0.034	0.182	0.231	0.253	0.296	0.327	0.189
DEM	−0.010	−0.016	0.068	0.071	0.101	0.123	0.152	0.109
SLOPE	−0.319	−0.325	−0.408	−0.394	−0.371	−0.339	−0.331	−0.249
ASPECT	−0.053	−0.055	0.208	0.181	0.165	0.166	0.150	0.156
FLOWACC	0.171	0.164	0.037	0.056	0.089	0.110	0.118	0.158

† Significant correlations are underlined.

Table 4. Inputs used for different models used for developing parametric and point PTFs.

Model	Inputs†
Model 01	ssc
Model 02	ssc-bd
Model 03	ssc-oc-bd
Model 04	ssc-ndvi
Model 05	ssc-bd-ndvi
Model 06	ssc-dem
Model 07	ssc-bd-dem
Model 08	ssc-slp
Model 09	ssc-bd-slp
Model 10	ssc-asp
Model 11	ssc-bd-asp
Model 12	ssc-flwa
Model 13	ssc-bd-flwa
Model 14	ssc-bd-dem-ndvi
Model 15	ssc-bd-slp-ndvi
Model 16	ssc-bd-asp-ndvi
Model 17	ssc-bd-flwa-ndvi
Model 18	ssc-bd-spl-asp-flwa-ndvi

† ssc, %sand-%silt-%clay; bd, bulk density; oc, organic C; slp, slope; asp, aspect; flaw, flow accumulation; dem, digital elevation model; ndvi, normalized different vegetation index.

showed significant correlations with basic soil properties and slope. Theoretically, this finding may reflect the significance of α (related to the bubbling pressure or biggest pore that may in turn be associated with relative landscape position) as opposed to n (related to entire pore-size distribution as per the textural composition). For all hydraulic parameters except α, basic soil properties (based on same support size) showed the most significant correlations. The low correlations of soil hydraulic parameters with topographic and vegetation attributes could be a result of different spatial resolution (support size) of topographic attributes (e.g., Famiglietti et al., 1998) and vegetation indices (NDVI) with respect to hydraulic properties measurement scale. The low correlations of topographic attributes with hydraulic parameters are in agreement with previous studies (Leij et al., 2004, Moore et al., 1993).

Table 3 shows correlations between predictors and water contents at different matric potentials. Most of the basic soil properties appear to be significantly correlated to water content at different matric potentials with exception to OC and water content at 3000 and 8000 cm and to bulk density and water content near saturation (5 and 10 cm). In particular, elevation (DEM) did not show any significant correlations to the water contents at any matric potentials as found in a previous study by Pachepsky et al. (2001). Slope showed significant correlations to water contents across the pressure range whereas flow accumulation and aspect could be correlated only to wet through intermediate range of water contents at (5 and 500 cm). NDVI was significantly correlated to water contents at matric potentials between 333 (i.e., field capacity) and 15000 cm (i.e., permanent wilting point). Note that this finding reconfirms our previous observation of significant correlation between NDVI and available water content (θ_{333}–θ_{15000}) for the plants.

Hydraulic Parameters

Hierarchical inputs used for different neural network models are shown in Table 4. Tables 5 and 6 show the correlations between the fitted and predicted hydraulic parameters and water contents at different matric potentials by the neural network models, respectively. In general, correlation coefficients were greater for the $\theta(h)$ than for (θ_r, θ_s, α, n). This observation may be due to the fitted nature of van Genuchten hydraulic parameters to the nonlinear $\theta(h)$ function. In addition, RMSE values for both hydraulic parameters and soil water content at different matric potentials are presented in Tables 7 and 8 illustrating the goodness of fit of individual neural network models. These are useful to quantify the uncertainty or the spread of the predicted data from the measured parameters and are useful for stochastic modeling of hydrologic processes.

Table 5. Correlation coefficients between the measured and the predicted hydraulic parameters.

Correlations	θ_r	θ_s	α	n
Model 01	0.487	0.708	0.445	0.531
Model 02	0.484	0.779	0.454	0.623
Model 03	0.547	0.860	0.491	0.662
Model 04	0.512	0.745	0.468	0.558
Model 05	0.632	0.764	0.472	0.682
Model 06	0.437	0.716	0.299	0.514
Model 07	0.526	0.794	0.356	0.652
Model 08	0.568	0.642	0.237	0.406
Model 09	0.559	0.774	0.397	0.572
Model 10	0.576	0.788	0.462	0.559
Model 11	0.554	0.750	0.423	0.589
Model 12	0.437	0.717	0.446	0.534
Model 13	0.437	0.859	0.514	0.579
Model 14	0.709	0.822	0.501	0.672
Model 15	0.739	0.761	0.516	0.601
Model 16	0.667	0.757	0.395	0.611
Model 17	0.511	0.815	0.453	0.603
Model 18	0.774	0.822	0.369	0.491

Using only the information from soil texture (Model 1) resulted in low correlation coefficients compared with the rest of the neural network models for all the hydraulic parameters (0.445 for α, 0.531 for n, 0.487 for θ_r, 0.708 for θ_s). Correlations increased from Model 1 to Model 3 for all the parameters except for θ_r where the correlation dropped statistically insignificantly from Model 1 to 2. The increase in correlation is due to increase in information regarding the PSD with the addition of OC and ρ_b. Addition of vegetation information (Models 4 and 5) also showed an increase in correlation compared with Models 1 and 2 for all parameters except for θ_s where

Table 6. Correlation coefficients between the measured and the predicted water contents.

Correlations	θ_5	θ_{10}	θ_{333}	θ_{500}	θ_{1000}	θ_{3000}	θ_{8000}	θ_{15000}
Model 01	0.451	0.461	0.653	0.684	0.662	0.662	0.636	0.574
Model 02	0.502	0.511	0.693	0.728	0.728	0.740	0.749	0.637
Model 03	0.499	0.504	0.676	0.723	0.711	0.710	0.700	0.569
Model 04	0.523	0.517	0.735	0.751	0.747	0.758	0.757	0.585
Model 05	0.558	0.563	0.767	0.788	0.784	0.797	0.808	0.636
Model 06	0.511	0.518	0.704	0.738	0.738	0.737	0.834	0.602
Model 07	0.524	0.530	0.720	0.731	0.728	0.719	0.831	0.592
Model 08	0.511	0.516	0.738	0.725	0.704	0.687	0.663	0.593
Model 09	0.563	0.564	0.752	0.763	0.746	0.720	0.714	0.603
Model 10	0.455	0.461	0.694	0.713	0.702	0.713	0.694	0.651
Model 11	0.529	0.537	0.769	0.775	0.759	0.752	0.742	0.703
Model 12	0.450	0.461	0.658	0.692	0.665	0.652	0.619	0.558
Model 13	0.481	0.492	0.698	0.737	0.712	0.689	0.670	0.596
Model 14	0.569	0.570	0.788	0.829	0.828	0.838	0.858	0.561
Model 15	0.592	0.592	0.778	0.800	0.783	0.767	0.767	0.632
Model 16	0.415	0.440	0.507	0.561	0.491	0.414	0.388	0.374
Model 17	0.564	0.562	0.794	0.796	0.795	0.795	0.800	0.652
Model 18	0.553	0.556	0.816	0.817	0.822	0.814	0.806	0.639

Table 7. Root Mean Square Error between the measured and the predicted hydraulic parameters.

RMSE	θ_r	θ_s	α	n
Model 01	0.037	0.05	0.006	0.67
Model 02	0.037	0.044	0.006	0.64
Model 03	0.036	0.039	0.005	0.55
Model 04	0.036	0.048	0.006	0.66
Model 05	0.033	0.046	0.006	0.54
Model 06	0.038	0.052	0.006	0.65
Model 07	0.036	0.043	0.006	0.59
Model 08	0.035	0.053	0.006	0.80
Model 09	0.035	0.046	0.006	0.60
Model 10	0.035	0.048	0.006	0.61
Model 11	0.035	0.048	0.006	0.61
Model 12	0.038	0.051	0.006	0.67
Model 13	0.038	0.039	0.005	0.68
Model 14	0.031	0.043	0.005	0.56
Model 15	0.030	0.047	0.005	0.59
Model 16	0.032	0.046	0.006	0.59
Model 17	0.026	0.043	0.006	0.61
Model 18	0.029	0.042	0.006	0.70

correlation dropped around 0.779 (Model 2) to 0.764 for θ_s (Model 5). Since NDVI does not show any significant correlation to any other input parameters, this suggests its high potential for being used as a predictor for the hydraulic parameters. Addition of topographic variables showed a mixed response for different hydraulic parameters. Adding elevation (DEM) as input (Model 6) to the soil texture resulted in a decrease in correlation coefficients for all parameters except for θ_s where a statistically insignificant increase in correlation (from 0.708 to 0.716) was observed. Effects of adding elevation (DEM) and the bulk density jointly (Model 7) showed increasing correlation trends for all parameters except for α as compared with Model 2. This finding suggests the significance of relative landscape position resulting from soil erosion/depositional patterns that in turn relates to the soil hydraulic properties. Adding slope as a predictor showed decreasing correlation trends for all the parameters as illustrated (Model 8 vs. 1 and 9 vs. 2) except for the parameter θ_r. One of the possible explanations for this behavior could be the generally low values of slope across the study area, which resulted in masking of the properties of the other input parameters. Addition of aspect to the inputs of Model 1 resulted in Model 10, which showed increasing correlation trends for all the hydraulic parameters. However, aspect along with bulk density (Model 11) resulted in lowering of correlation coefficients of all the hydraulic parameters except for θ_r when compared with Model 2. Including flow accumulation information resulted in mixed model performances for various hydraulic parameters (Model 12 vs. 1 and 13 vs. 2).

Different combinations of topographic and vegetation information (Model 14 to 17) produced different model performance. Combining elevation and NDVI inputs together in Model 14 showed increased correlation coefficients for all the hydraulic parameters except for *n* when compared with Model 5 and 7. Combination of flow accumulation and NDVI (Model 17) on the other hand showed decreased correlations for all the hydraulic parameters. For slope and aspect combinations with NDVI (Model 15 and 16), the correlation coefficients increased for θ_r, θ_s, and α when compared with Model 2. Although the results of including topographic and vegetation parameters were mixed for individual combinations, a general increase was observed in correlations in comparison with other models without these inputs.

Combination of all the inputs together (Model 18) showed the maximum correlation coefficient for the residual water content (θ_r) with respect to all the neural network models. For water content at saturation (θ_s) performance of Model 18 was moderate, whereas the model showed poorest performance for predicting α and *n*. This could be the result of over-parameterization of Model 18 because of maximum number of inputs used.

Table 8. Root Mean Square Errors between the measured and the predicted water contents.

RMSE	θ_5	θ_{10}	θ_{333}	θ_{500}	θ_{1000}	θ_{3000}	θ_{8000}	θ_{15000}
Model 01	0.029	0.029	0.051	0.051	0.052	0.051	0.050	0.049
Model 02	0.028	0.028	0.048	0.047	0.047	0.045	0.044	0.047
Model 03	0.028	0.028	0.049	0.048	0.048	0.048	0.046	0.049
Model 04	0.028	0.028	0.044	0.044	0.043	0.042	0.043	0.049
Model 05	0.027	0.027	0.042	0.042	0.039	0.039	0.039	0.047
Model 06	0.028	0.027	0.046	0.044	0.046	0.047	0.038	0.048
Model 07	0.028	0.027	0.045	0.047	0.047	0.047	0.039	0.049
Model 08	0.028	0.028	0.043	0.047	0.048	0.049	0.048	0.048
Model 09	0.027	0.026	0.043	0.043	0.045	0.047	0.046	0.048
Model 10	0.029	0.028	0.048	0.048	0.049	0.048	0.046	0.045
Model 11	0.028	0.027	0.041	0.042	0.043	0.042	0.045	0.043
Model 12	0.029	0.028	0.049	0.049	0.051	0.052	0.051	0.050
Model 13	0.029	0.028	0.046	0.045	0.048	0.048	0.047	0.048
Model 14	0.027	0.026	0.041	0.036	0.036	0.030	0.037	0.050
Model 15	0.027	0.026	0.041	0.039	0.042	0.041	0.043	0.048
Model 16	0.047	0.045	0.062	0.058	0.061	0.063	0.061	0.061
Model 17	0.027	0.027	0.039	0.039	0.039	0.040	0.041	0.044
Model 18	0.027	0.027	0.037	0.037	0.038	0.039	0.040	0.046

Volumetric Water Content at Different Matric Potentials

In general, performance of neural network models for water contents at different matric potential $\theta(h)$ were better than for the hydraulic parameters (Tables 5 vs. 6 and 7 vs. 8). This behavior reflects the fact water contents are directly measured and are not fitted parameters as the hydraulic parameters. The correlation coefficients for all the models were relatively small at the wet end (matric potentials of 5 and 10 cm) and at the dry end (matric potential 15000 cm) of the soil water retention curve. The maximum correlations were observed at the intermediate matric potential range for all the models. This feature may reflect the nonlinearity and change in slope of $\theta(h)$ and thus its sensitivity to model inputs across the matric potential range (h). Addition of topographic, vegetation or combination of topographic and vegetation information resulted in increased correlation coefficients for all models, compared with models using only the basic soil properties (Model 1 through Model 3). Exceptions to these observations were Model 12 and Model 13 with flow accumulation as input, in which the performance decreased for matric potentials at 5, 3000, and 8000 cm. Using all the input parameters together in Model 18 did not result in maximum correlation coefficients for the water contents $\theta(h)$ which could again be attributed to possible over-parametrizing of the models.

Combination of topographic attributes and vegetation information produced mixed effect on model performance. For example, Model 16 with the combination of

Table 9. 90% Confidence intervals of the hydraulic parameters using Bootstrap Technique.

	θ_r		θ_s		α		n	
	Lower	Upper	Lower	Upper	Lower	Upper	Lower	Upper
Model 01	0.05740	0.10733	0.34146	0.39245	0.01101	0.01986	1.24858	2.32331
Model 02	0.06340	0.10348	0.34682	0.39001	0.01067	0.02038	1.36729	2.34242
Model 03	0.06274	0.10685	0.34601	0.38828	0.01172	0.01982	1.42664	2.35241
Model 04	0.06405	0.09982	0.35072	0.38745	0.01105	0.01965	1.43293	2.19218
Model 05	0.06252	0.10768	0.35010	0.38954	0.01193	0.01905	1.43703	2.17430
Model 06	0.06246	0.10853	0.34306	0.39140	0.01267	0.01936	1.42542	2.18157
Model 07	0.06734	0.10249	0.34896	0.38706	0.01342	0.01871	1.45518	2.19390
Model 08	0.06101	0.10960	0.34510	0.39117	0.01106	0.01980	1.41767	2.30932
Model 09	0.06345	0.10585	0.34845	0.39084	0.01154	0.01866	1.39848	2.29406
Model 10	0.06104	0.10856	0.34606	0.38923	0.01148	0.01947	1.29616	2.27060
Model 11	0.06732	0.10440	0.34548	0.38956	0.01123	0.01876	1.35747	2.28342
Model 12	0.06107	0.10999	0.34368	0.39284	0.01114	0.02001	1.24426	2.34226
Model 13	0.06470	0.10415	0.35068	0.39228	0.01056	0.02000	1.35832	2.28853
Model 14	0.06814	0.10220	0.35503	0.38938	0.01281	0.01960	1.48562	2.21543
Model 15	0.06927	0.09847	0.35238	0.38968	0.01321	0.01881	1.51927	2.15137
Model 16	0.05745	0.11093	0.34326	0.39452	0.01057	0.02020	1.29176	2.34584
Model 17	0.06732	0.10440	0.35298	0.38747	0.01243	0.01902	1.38253	2.05260

NDVI and aspect produced poorer correlations compared with the models using these inputs individually along with basic soil properties (Model 4 and 10). In contrast Model 14 with elevation and NDVI as inputs performs better as compared with Model 5 and 7 for water content at all matric potentials except at 15000 cm. Correlations dropped in the dry range (1000 to 15000 cm) using slope and NDVI as input (Model 15). Model 17 with flow accumulation and NDVI gave intermediate correlation coefficients for water content at the matric potentials of 100, 3000, and 8000 cm.

For hydraulic parameters as well as soil water content at different matric potentials, RMSE shows the same trends as shown by the correlation coefficients, lower RMSE were obtained with higher correlations. Model performance (correlation coefficient or RMSE) depends on different input parameters and their correlations between each other. The maximum number of input parameters did not necessarily result in the best model performance and hence care has to be taken while choosing the different predictors. Not a single individual neural network model was able to produce the best result for all the output variables. This suggests that to obtain the best possible estimation, different combinations of input parameters have to be used for different output variables. The use of ancillary topographic and vegetation data has been found helpful to increase the correlation coefficients for soil hydraulic properties but a general trend is hard to establish. Although physical reasoning/understanding for these findings can at best be speculative at present, further designed experiments isolating specific attribute combinations could help unravel the intricate relationships between specific soil, topography, and vegetation properties at different scales.

Uncertainty Analysis

Results indicated considerable uncertainties in predicted output variables as observed in other studies (e.g., Schaap et al., 1998). Table 9 and 10 show the 5 (lower) and 95 (upper) percentiles from bootstrapping of the replicate estimates for hydraulic parameters and water contents at different matric potentials. The range between two percentiles represents the general spread or uncertainties of the model predictions. For the hydraulic parameters, the uncertainty levels varied proportional to the magnitude of the parameter (e.g., n vs. α). A general decrease in the uncertainty values are observed with the corresponding hierarchical increase in inputs except for models with flow accumulation as input. Although the

Table 10. 90% Confidence intervals of the predicted water contents at different matric potentials predicted using Bootstrap Technique.

	θ_5		θ_{10}		θ_{333}		θ_{500}		θ_{1000}		θ_{3000}		θ_{8000}		θ_{15000}	
	Lower	Upper	Lower	Upper	Lower	Upper	Lower	Upper	Lower	Upper	Lower	Upper	Lower	Upper	Lower	Upper
Model 01	0.3204	0.3893	0.3185	0.3871	0.1915	0.2512	0.1732	0.2287	0.1482	0.1981	0.1194	0.1631	0.0707	0.1781	0.0688	0.1770
Model 02	0.3206	0.3888	0.3188	0.3867	0.1955	0.2552	0.1775	0.2329	0.1526	0.2022	0.1232	0.1666	0.0756	0.1800	0.0700	0.1826
Model 03	0.3210	0.3890	0.3192	0.3867	0.1945	0.2519	0.1767	0.2300	0.1514	0.1990	0.1218	0.1635	0.0807	0.1704	0.0737	0.1741
Model 04	0.3212	0.3891	0.3194	0.3868	0.1962	0.2543	0.1781	0.2321	0.1528	0.2013	0.1233	0.1660	0.0776	0.1773	0.0766	0.1734
Model 05	0.3215	0.3898	0.3197	0.3876	0.1979	0.2568	0.1797	0.2345	0.1545	0.2037	0.1248	0.1678	0.0782	0.1796	0.0730	0.1785
Model 06	0.3211	0.3896	0.3193	0.3873	0.1953	0.2544	0.1771	0.2320	0.1519	0.2013	0.1224	0.1658	0.0751	0.1791	0.0711	0.1759
Model 07	0.3190	0.3861	0.3172	0.3840	0.1931	0.2490	0.1751	0.2268	0.1502	0.1965	0.1212	0.1621	0.0820	0.1680	0.0796	0.1668
Model 08	0.3208	0.3896	0.3190	0.3874	0.1967	0.2568	0.1782	0.2341	0.1530	0.2032	0.1232	0.1671	0.0732	0.1820	0.0682	0.1820
Model 09	0.3207	0.3887	0.3189	0.3864	0.1947	0.2527	0.1764	0.2302	0.1516	0.1999	0.1224	0.1649	0.0781	0.1752	0.0708	0.1773
Model 10	0.3206	0.3889	0.3186	0.3865	0.1910	0.2492	0.1726	0.2265	0.1474	0.1958	0.1184	0.1608	0.0741	0.1716	0.0724	0.1713
Model 11	0.3200	0.3875	0.3181	0.3852	0.1920	0.2497	0.1740	0.2274	0.1490	0.1968	0.1200	0.1620	0.0775	0.1708	0.0733	0.1745
Model 12	0.3207	0.3894	0.3188	0.3872	0.1960	0.2561	0.1775	0.2334	0.1520	0.2023	0.1223	0.1665	0.0709	0.1833	0.0686	0.1807
Model 13	0.3219	0.3897	0.3200	0.3875	0.1944	0.2530	0.1765	0.2309	0.1514	0.2003	0.1218	0.1648	0.0751	0.1764	0.0693	0.1779
Model 14	0.3204	0.3873	0.3185	0.3850	0.1952	0.2516	0.1767	0.2287	0.1511	0.1976	0.1215	0.1624	0.0836	0.1663	0.0754	0.1710
Model 15	0.3218	0.3890	0.3199	0.3868	0.1965	0.2542	0.1781	0.2316	0.1529	0.2008	0.1235	0.1655	0.0805	0.1738	0.0735	0.1774
Model 16	0.1940	0.5237	0.1947	0.5236	0.0134	0.2185	−0.004	0.1869	−0.048	0.1151	−0.093	0.0344	−0.098	0.0125	−0.044	0.0476
Model 17	0.3220	0.3898	0.3202	0.3875	0.1948	0.2521	0.1767	0.2299	0.1516	0.1991	0.1222	0.1639	0.0804	0.1710	0.0747	0.1722

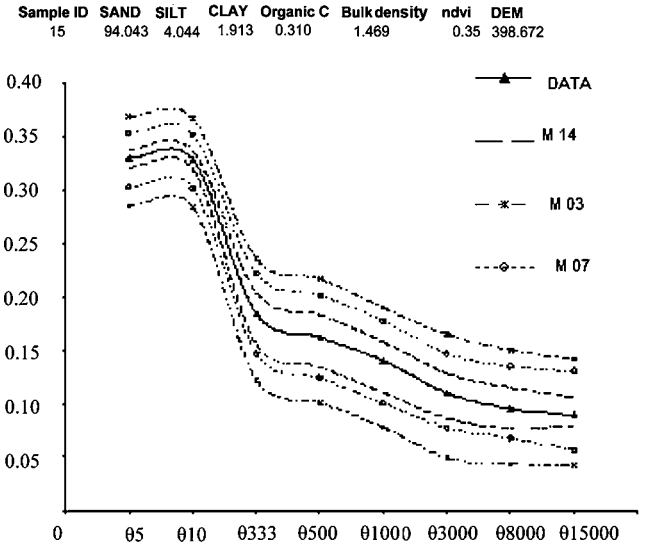

Fig. 3. Lower and upper confidence intervals of three different neural network models for water content at different matric potentials.

results from correlation coefficients and RMSE are not exactly replicated for all the bootstrap sets generated, the general trends of uncertainties observed are in agreement to the results discussed in the previous sections. For water contents, all the models show large spreads at the wet end (matric potentials of 5 and 10 cm) and at the dry end (matric potential 15000 cm) of the soil water retention curve, which is also supported by the small correlation coefficients obtained at these potentials. Using only the basic soil properties resulted in generally large ranges for water content at the small and large matric potentials and small ranges for water content at intermediate matric potentials of the water retention curves. Note that joint inclusion of elevation and NDVI as predictors (Model 14) gave lowest while joint inclusion of aspect and NDVI as predictors (Model 16) gave highest uncertainty (range) consistently for all the matric potentials. Mixed model responses were obtained for the other combinations of topographic attributes and vegetation information with the basic soil properties. Figure 3 shows the water contents at different matric potentials obtained from the Models 3, 7, and 14 along with the lab measurements for one soil sample (Sample ID # 15) from the validation data set. The result clearly demonstrates the reduction in the uncertainty levels with the addition of elevation and NDVI as inputs. However, statistical comparison (one way ANOVA test at significance level $\alpha = 0.05$) of the bootstrapped replications between the four neural network models (1, 3, 7, and 14) showed insignificant differences with a range of statistical power/confidence (0.236–0.999; see Table 11).

Application of the Neural Network Models

Neural network Model 14 (%sand-%silt-%clay-bulk density-DEM-NDVI) and Model 1 (%sand-%silt-%clay) were used to generate hydraulic parameter maps for the LW watershed of the study region at 1 km spatial resolution. The values for %sand, %silt, and %clay were obtained from the STATSGO database (1: 250000 scale). Elevation and NDVI values were obtained from DEM and the clipped NDVI images of 30 m resolution. A pixel scale of 1 km was chosen to overcome the resolution mismatch between the different inputs used. The output hydraulic parameters for LW watershed were generated using the weights assigned to the model inputs after training.

Figure 4 shows the estimated hydraulic parameters (θ_r, θ_s, α, n) from Model 1. The watershed is divided into zones that correspond to the soil mapping units of STATSGO database. Each map unit represents a unique value of sand, silt and clay percentages and hence only a single estimate of hydraulic parameters could be obtained for each zone. The estimated hydraulic parameters from Model 14 (Fig. 5, averaged over 800 m × 800 m pixels matching the air-borne passive microwave remote sensor footprints used during SGP97 experiment) exhibit a wider range compared with those generated from Model 1. This is due to the fine resolution of topography and vegetation inputs compared with the basic soil properties. The variation within soil mapping units of the estimated hydraulic parameters is visible due to the fine resolution and the indirect effects of the ancillary topography and vegetation parameters.

CONCLUSIONS

Vegetation and topography have been known to affect the soil hydrologic phenomena and properties. This study was designed to examine the effect of including topographic and vegetation attributes on the prediction

Table 11. Statistical significance (of similarity) between predictions using four different neural network models at $\alpha = 0.05$ (with one-way ANOVA test).

	θ_r				θ_s				α				n				θ_5				θ_{10}			
Model	**1**	**3**	**7**	**14**	**1**	**3**	**7**	**14**	**1**	**3**	**7**	**14**	**1**	**3**	**7**	**14**	**1**	**3**	**7**	**14**	**1**	**3**	**7**	**14**
1	**1**	**0.874**	**0.780**	**0.873**	**1**	**0.741**	**0.798**	**0.694**	**1**	**0.236**	**0.569**	**0.498**	**1**	**0.339**	**0.976**	**0.642**	**1**	**0.973**	**0.651**	**0.843**	**1**	**0.975**	**0.655**	**0.838**
3		**1**	**0.904**	**0.999**		**1**	**0.940**	**0.950**		**1**	**0.537**	**0.611**		**1**	**0.355**	**0.623**		**1**	**0.627**	**0.822**		**1**	**0.633**	**0.814**
7			**1**	**0.905**			**1**	**0.890**			**1**	**0.914**			**1**	**0.664**			**1**	**0.794**			**1**	**0.808**
14				**1**				**1**				**1**				**1**				**1**				**1**
	θ_{333}				θ_{500}				θ_{1000}				θ_{3000}				θ_{8000}				θ_{15000}			
Model	**1**	**3**	**7**	**14**	**1**	**3**	**7**	**14**	**1**	**3**	**7**	**14**	**1**	**3**	**7**	**14**	**1**	**3**	**7**	**14**	**1**	**3**	**7**	**14**
1	**1**	**0.865**	**0.980**	**0.851**	**1**	**0.831**	**0.998**	**0.877**	**1**	**0.855**	**0.988**	**0.915**	**1**	**0.833**	**0.963**	**0.939**	**1**	**0.905**	**0.949**	**0.955**	**1**	**0.902**	**0.973**	**0.971**
3		**1**	**0.846**	**0.986**		**1**	**0.829**	**0.954**		**1**	**0.867**	**0.939**		**1**	**0.920**	**0.944**		**1**	**0.956**	**0.950**		**1**	**0.929**	**0.931**
7			**1**	**0.831**			**1**	**0.875**			**1**	**0.927**			**1**	**0.976**			**1**	**0.995**			**1**	**0.998**
14				**1**				**1**				**1**				**1**				**1**				**1**

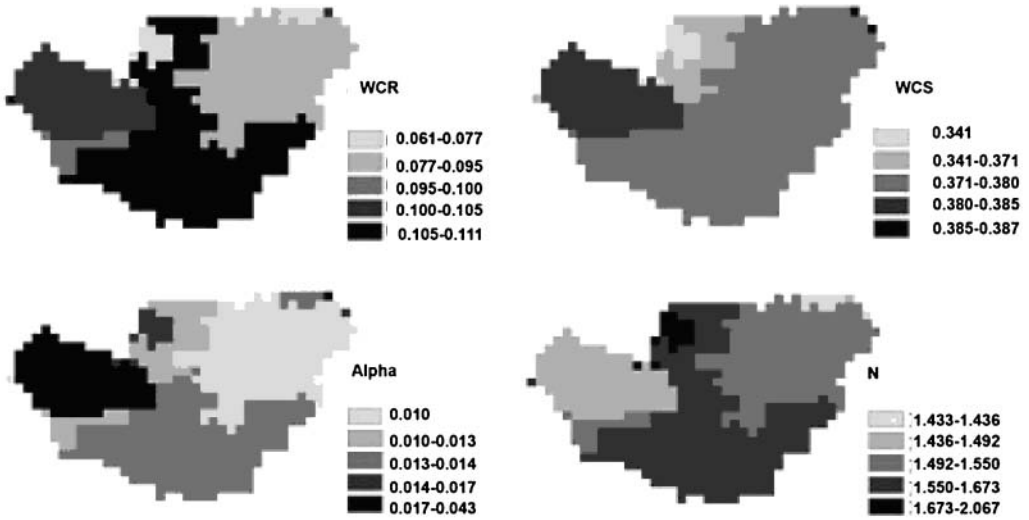

Fig. 4. Predictions of van Genuchten hydraulic parameters based on Model 1.

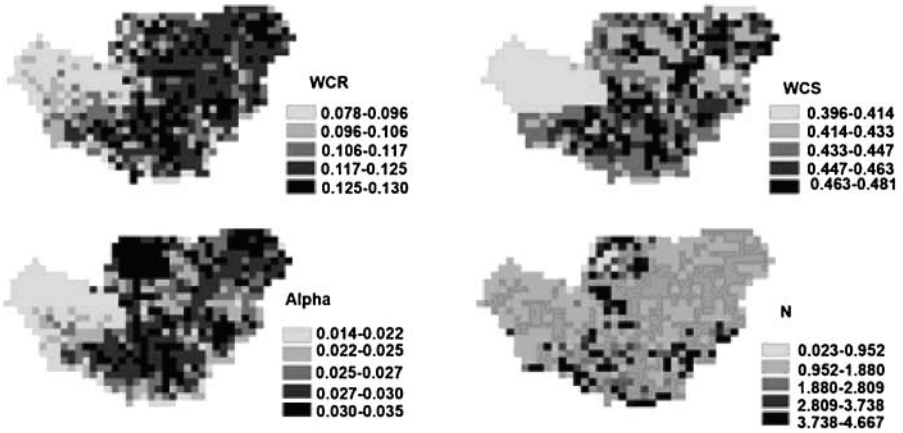

Fig. 5. Predictions of van Genuchten hydraulic parameters based on Model 14.

of near-surface soil hydraulic properties. Specifically, we explored the usefulness of topographic attributes from DEM and remotely sensed NDVI in addition to soil physical attributes in developing and improving catchment- or regional-scale PTFs where vegetation cover is dominantly perennial. Artificial neural networks were used to develop 18 models to predict the van Genuchten hydraulic parameters (θ_r, θ_s, α, n) and water contents at different matric potentials, $\theta(h)$. Improvements (of different statistical significance) were found for certain soil water retention parameters and soil water contents using different combinations of basic soil properties along with topography and vegetation attributes as inputs. The pixel-scale hydraulic parameters predicted using the developed models demonstrate the usefulness of incorporating topographic and vegetation information along with the basic soil properties. Although, the basic soil properties showed the maximum correlation to the hydraulic parameters, the spatial resolution of available soil data is usually not suitable enough for distributed hydrologic modeling at watershed or regional scale. The indirect influence of topographic and vegetation properties on soil hydraulic properties, and their availability at finer resolution using advanced ground/remote sensing techniques (e.g., DEM and NDVI) demonstrate the suitability of developing PTVTFs at the landscape scales. The addition of the remotely sensed NDVI has been found useful in increasing the correlation coefficients for soil hydraulic properties, although a conclusive trend is hard to establish. Further studies isolating specific attribute combinations could help unravel the intricate relationships between specific soil, topography, and vegetation properties at different scales.

ACKNOWLEDGMENTS

Funding support from NASA grant (NAG5-11702), NASA fellowship (ESSF/03-000-0191) to Sanjay Sharma, and NSF-SAHRA is acknowledged.

REFERENCES

Allen, P.B., and J.W. Naney. 1991. Hydrology of Little Washita River Watershed. Oklahoma: data and analyses. USDA, ARS 90. U. S. Gov. Print Office. Washington, DC.

Ahuja, L.R., J.W. Naney, and R.D. Williams. 1985. Estimating soil water characteristics from simpler properties or limited data. Soil Sci. Soc. Am. J. 49:1100–1105.

Brooks, R.H., and A.T. Corey. 1964. Hydraulic properties of porous media hydrology paper no. 3. Colorado State Univ, Fort Collins, CO.

Campbell, G.S. 1974. A simple method for determining unsaturated hydraulic conductivity from moisture retention data. Soil Sci. 177: 311–314.

Clapp, R.B., and G.M. Hornberger. 1978. Empirical equations for some hydraulic properties. Water Resour. Res. 14:601–604.

Dennis, J.E., D.M. Gay, and R.E. Welsch. 1981. NL2SOL: An adaptive nonlinear least squares algorithm. ACM Trans. Math. Softw. 7:348–368.

Efron, B., and R.J. Tibshirani. 1993. An introduction to the bootstrap. Monographs on statistics and applied probability. Chapman and Hall, New York.

Famiglietti, J.S., J.W. Rudnicki, and M. Rodell. 1998. Variability in surface moisture content along a hillslope transect: Rattlesnake Hill, Texas. J. Hydrol. 210:259–281.

Famiglietti, J.S., J.A. Devereux, C.A. Laymon, T. Tsegaye, P.R. Houser, T.J. Jackson, S.T. Graham, and M. Rodell. 1999. Ground-based investigation of soil moisture variability within remote sensing footprints during the Southern Great Plains 1997 (SGP97). Hydrology Experiment. Water Resour. Res. 35:1839–1851.

Gee, G.W., and J.W. Bauder. 1986. Particle-size analysis. p. 383–411. *In* A. Klute (ed.) Methods of soil analysis. Part 1. 2nd ed. Agron. Monogr. No. 9. ASA and SSSA, Madison, WI.

Hawley, M.E., T.J. Jackson, and R.H. McCuen. 1983. Surface soil moisture variation on small agricultural watersheds. J. Hydrol. 62:179–200.

Jackson, T.J., and F.R. Schiebe. 1993. "Hydrology data report Washita '92," NAWQL 93–1, USDA.

Koekkoek, E.J.W., and H.W.G. Booltink. 1999. Neural network models to predict soil water retention. Eur. J. Soil Sci. 50:489–495.

Leij, F.J., N. Romano, M. Palladino, and M.G. Schaap. 2004. Topographical attributes to predict soil hydraulic properties along a hillslope transect. Water Resour. Res. 40:1–15.

Minasny, B., and A.B. McBratney. 2002. The neuro-m method for fitting neural network parametric pedotransfer functions. Soil Sci. Soc. Am. J. 66:352–361.

Mohanty, B.P., P.J. Shouse, D.A. Miller, and M.Th. van Genuchten. 2002. Soil property database: Southern Great Plains 1997 Hydrology Experiment. Water Resour. Res. 28:1–8.

Mohanty, B.P., and T.H. Skaggs. 2001. Spatio-temporal evolution and time-stable characteristic of soil moisture within remote sensing footprints with varying soil. slope, and vegetation. Adv. Water Res. 24:1051–1067.

Mohanty, B.P., T.H. Skaggs, and J.S. Famiglietti. 2000. Analysis and mapping of field-scale soil moisture variability using high resolution ground based data during the southern Great Plains 1997 (SGP97) hydrology experiment. Water Resour. Res. 36:1023–1031.

Moore, I.D., P.E. Gessler, G.A. Nielsen, and G.A. Peterson. 1993. Soil attribute prediction using terrain analysis. Soil Sci. Soc. Am. J. 57: 443–452.

Pachepsky, Ya.A., W.J. Rawls, and D.J. Timlin. 1999. The current status of pedotransfer functions, their accuracy, reliability, and utility in field- and regional-scale modeling. p. 223–234. *In* D.L. Corwin et al. (ed.) Assessment of non-point source pollution in the vadose zone. Geophysical Monogr. 108. American Geophysical Union, Washington, DC.

Pachepsky, Ya.A., D.J. Timlin, and W.J. Rawls. 2001. Soil water retention as related to topographic variables. Soil Sci. Soc. Am. J. 65:1787–1795.

Pachepsky, Ya.A., D. Timlin, and G. Várallyay. 1996. Artificial neural networks to estimate soil water retention from easily measurable data. Soil Sci. Soc. Am. J. 60:727–773.

Rawls, W.J., D.L. Brakensiek, and K.E. Saxton. 1982. Estimation of soil water properties. Trans. ASAE 25:1316–1320.

Rawls, W.J., T.J. Gish, and D.L. Brakensiek. 1991. Estimating soil water retention from soil physical properties and characteristics. Adv. Soil Sci. 16:213–234.

Reynolds, S.G. 1970. The gravimetric method of soil moisture determination, part III. An examination of factors influencing soil moisture variability. J. Hydrol. 11:288–300.

Schaap, M.G., F.J. Leij, and M.Th. van Genuchten. 1998. Neural network analysis for hierarchical prediction of soil hydraulic properties. Soil Sci. Soc. Am. J. 62:847–855.

Southern Great Plains 1997 Science Team, Southern Great Plains '97 (SGP97) data archive. Available online at http://daac.gsfc.nasa.gov/fieldexp/SGP97/ (verified 15 May 2005), NASA-GSFC DAAC, Greenbelt, MD., 1997.

Tomasella, J., M.G. Hodnett, and L. Rossato. 2000. Pedotransfer functions for the estimation of soil water retention in Brazilian soils. Soil Sci Soc. Am. J. 64:327–338.

Tomasella, J., Ya. A. Pachepsky, S. Crestana, and W. J. Rawls. 2003. Comparison of two techniques to develop pedotransfer functions for water retention. Soil Sci Soc. Am. J. 44:1085–1092.

van Genuchten, M.Th. 1980. A closed-form equation for predicting the hydraulic conductivity of unsaturated soils. Soil Sci. Soc. Am. J. 44:892–898.

van Genuchten, M.Th., and F.J. Leij. 1992. On estimating the hydraulic properties of unsaturated soils. p. 1–14. *In* M.Th.Van Genuchten et al. (ed.) Indirect methods for estimating the hydraulic properties of unsaturated soils. Proceedings of the International Workshop on Indirect Methods for Estimating the Hydraulic Properties of Unsaturated Soils, Riverside, California, 11–13 October 1989. University of California, Riverside.

Vereecken, H., J. Maes, J. Feyen, and P. Darius. 1989. Estimating the soil moisture retention characteristics from texture, bulk density, and carbon content. Soil Sci. Soc. Am. J. 1484:389–403.

Wösten, J.H.M., Ya., A. Pachepsky, and W.J. Rawls. 2001. Pedotransfer functions: Bridging the gap between available basic soil data and missing soil hydraulic characteristics. J. Hydrol. 251:123–150.